Fish and Shellfish Immunology 89 (2019) 537–547

Contents lists available at ScienceDirect

Fish and Shellfish Immunology

journal homepage: www.elsevier.com/locate/fsi

Full length article

N-linked glycosylation sites in G protein of infectious hematopoietic necrosis virus (IHNV) affect its virulence and immunogenicity in rainbow trout

Shuo Jia[a,1], Guojie Ding[a,1], Chao Wang[a,c,1], Baohua Feng[a], Zhuo Wang[a], Li Wang[a], Yanping Jiang[a], Wen Cui[a], Xinyuan Qiao[a], Lijie Tang[a,b], Yijing Li[a,b,*], Yigang Xu[a,b,**]

[a] Heilongjiang Key Laboratory for Animal Disease Control and Pharmaceutical Development, College of Veterinary Medicine, Northeast Agricultural University, Harbin, PR China
[b] Northeastern Science Inspection Station, China Ministry of Agriculture Key Laboratory of Animal Pathogen Biology, Harbin, PR China
[c] Key Laboratory of Special Animal Epidemic Disease, Ministry of Agricultural, Institute of Special Economic Animal and Plant Sciences, Chinese Academy of Agricultural Sciences, Changchun, PR China

ARTICLE INFO

Keywords:
Infectious hematopoietic necrosis virus (IHNV)
G protein
Glycosylation
Viral virulence and immunogenicity

ABSTRACT

Infectious hematopoietic necrosis virus (IHNV) causes infectious hematopoietic necrosis in salmonid fish, resulting in substantial economic losses to the aquaculture industry worldwide. The G protein, which harbors the major antigenic determinants of IHNV, is an envelope glycoprotein that plays an important role in both pathogenicity and immunogenicity of IHNV. Previous studies have demonstrated that changes to viral glycosylation sites may affect replication and immunogenicity, but little is known about the specific contributions of G protein glycosylation to IHNV replication and pathogenicity. In this study, we predicted four N-linked glycosylation sites at position 56, 379, 401, and 438 Asp (N) in G protein, and using a reverse genetics system developed in our laboratory, constructed nine recombinant viruses with single, triple, or quadruple glycosylation site disruptions using alanine substitutions in the following combinations: rIHNV-N56A, rIHNV-N379A, rIHNV-N401A, rIHNV-N438A, rIHNV-N56A-N379A-N401A, rIHNV-N56A-N379A-N438A, rIHNV-N56A-N401A-N438A, rIHNV-N379A-N401A-N438A, and rIHNV-N56A-N379A-N401A-N438A. Our results confirmed that all four asparagines are sites of N-linked glycosylation, and Western blot confirmed that mutation of each predicted N-glycosylation sited impaired glycosylation. Among the nine recombinant IHNVs, replication levels decreased significantly *in vitro* and *in vivo* in the triple and quadruple mutants that combined mutation of asparagines 401 and 438, indicating the importance of glycosylation at these sites for efficient replication. Moreover, juvenile rainbow trout mortality after challenge by each of the nine mutants showed that, while eight mutants suffered almost 100% cumulative mortality over 30 days, the mutant with a single alanine substitution at position 438 resulted in cumulative mortality of less than 50% over 30 days. This mutant also elicited specific anti-IHNV IgM production earlier than other mutants, suggesting that glycosylation of asparagine 438 may be important for viral immune escape. In conclusion, our study reveals the effect of G protein glycosylation on the pathogenicity and immunogenicity of IHNV and provides a foundation for developing a live-attenuated vaccine.

1. Introduction

Infectious hematopoietic necrosis (IHN) is an infectious disease observed in salmonid fish, including trout and salmon, caused by infectious hematopoietic necrosis virus (IHNV). First reported in the United States, IHN is now widespread across the Pacific coast of Canada and the United States, Europe, and Asia, resulting in economic losses to the aquaculture industry worldwide [1–3]. Salmonid fish can be infected with IHNV from water contaminated by viral shedding in feces, urine, sexual fluids, and external mucus. Although many IHN vaccines are in development, only “APEX-IHN”, a nucleic acid vaccine developed by Novartis Animal Health, has been licensed in Canada [4]. IHNV,

* Corresponding authors. Heilongjiang Key Laboratory for Animal Disease Control and Pharmaceutical Development, College of Veterinary Medicine, Northeast Agricultural University, Harbin, PR China.
** Corresponding author. Heilongjiang Key Laboratory for Animal Disease Control and Pharmaceutical Development, College of Veterinary Medicine, Northeast Agricultural University, Harbin, PR China.
E-mail addresses: yijingli@163.com (Y. Li), yigangxu_china@sohu.com (Y. Xu).
[1] Shuo Jia, Guojie Ding, and Chao Wang contributed equally to this work.

https://doi.org/10.1016/j.fsi.2019.04.038
Received 14 December 2018; Received in revised form 7 April 2019; Accepted 11 April 2019
Available online 13 April 2019
1050-4648/

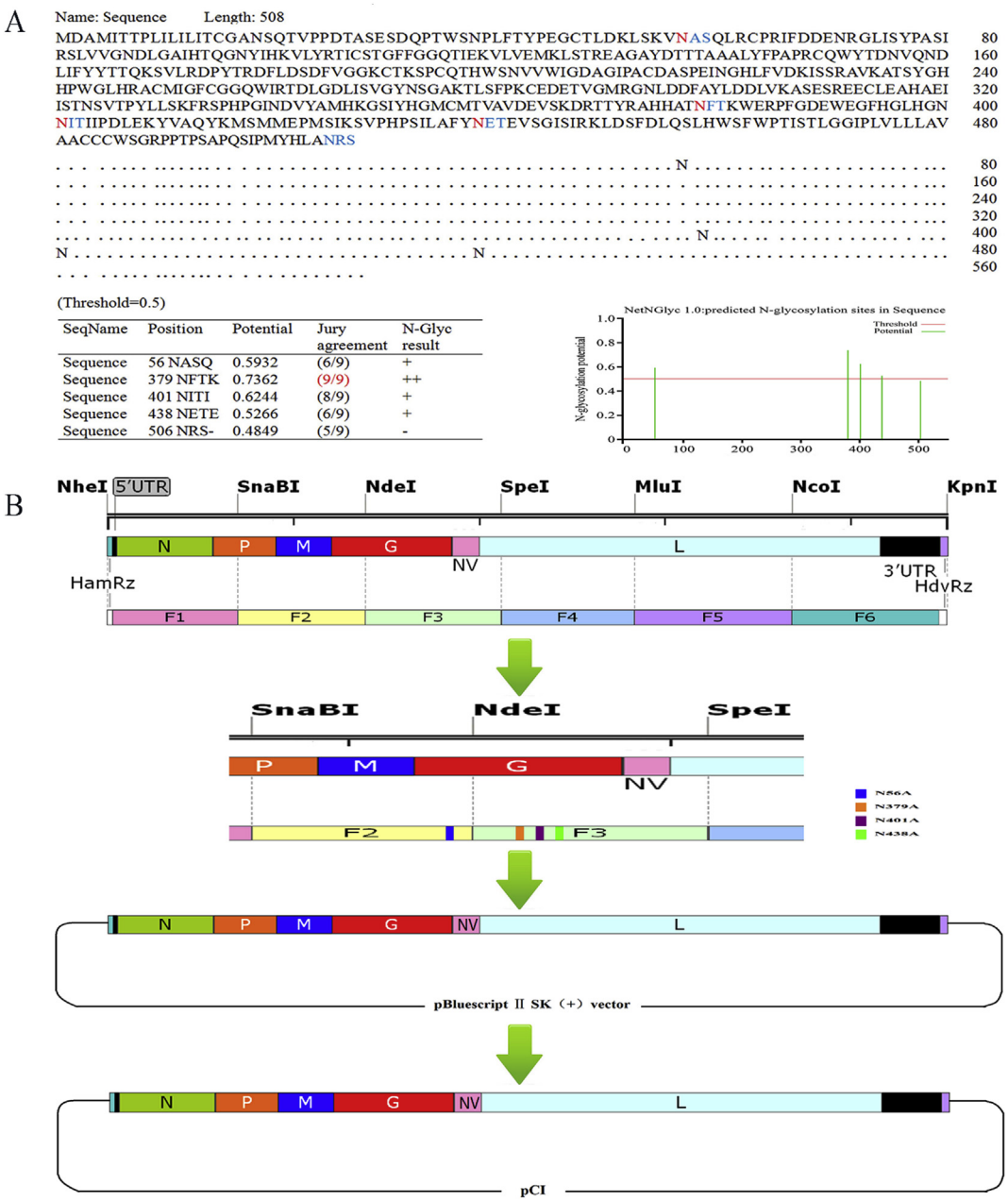

Fig. 1. Construction strategy of recombinant viruses. (A) The NetNGlyc 1.0 Server predicted potential N-linked glycosylation sites at residues 56, 379, 401, and 438 in the G protein of infectious hematopoietic necrosis virus (IHNV). (B) Strategy for construction of full-length recombinant viral genomes with G protein glycosylation site mutations, producing pCI-N56A, pCI-N379A, pCI-N401A, pCI-N438A, pCI-N56A-N379A-N401A, pCI-N56A-N379A-N438A, pCI-N56A-N401A-N438A, pCI-N379A-N401A-N438A, and pCI-N56A-N379A-N401A-N438A.

belonging to the *Novirhabdovirus* genus of the family *Rhabdoviridae*, is bullet-shaped and harbors an approximately 11 kb-long, single-stranded, negative-sense RNA genome. Its genome encodes a nucleocapsid protein (N), followed by a phosphoprotein (P), matrix protein (M), surface glycoprotein (G), non-virion protein (NV), and finally a RNA-dependent RNA polymerase (L) [5–8].

The surface-exposed structural G protein, an envelope glycoprotein, features the major antigenic determinants of IHNV and plays an important role in virus infection and invasion. The G protein is also an important immune protective antigen that can induce effective humoral and cellular immunity [9–11]. Many important antigenic epitopes in the G protein have been identified, including amino acids 78–81, 218–232, 272–276, 301–325, and 419–444 [12–14], of which all but 218–232 are neutralizing antigen epitopes; furthermore, mutations at positions 78, 218, 276 or 419 reduce IHNV virulence [12]. The importance of the G protein in IHNV pathogenicity and immunogenicity therefore suggest it as a promising candidate antigen for development of nucleic acid or subunit vaccines.

Glycosylation of envelope proteins is common to enveloped viruses, and is important for regulating replication of viruses including St. Louis encephalitis virus, dengue virus, yellow head virus, and classical swine fever virus. Changes to glycosylation sites could affect the folding and conformation of viral envelope proteins, thereby affecting viral replication and immunogenicity *in vivo* [15–18]. Indeed, N-linked glycosylation is essential for the correct folding and functioning of many proteins and is crucial for many enveloped viruses such as Hantaan and influenza viruses; in these viruses increased envelope protein glycosylation is important for binding to receptors, membrane fusion and cell entry, intracellular transport, virulence, and viral budding [19–21]. Moreover, the glycosylation of viral outer membrane proteins can mask

antigenic viral epitopes to prevent the host from producing specific antibodies, leading to viral immune escape and continuous infection [22–24]. Little, however, is known about the locations and relative contributions of G protein glycosylation sites on viral replication and pathogenicity, crucial information for targeted vaccine development.

Here, in order to explore the contributions of different G protein glycosylation sites to IHNV virulence and immunogenicity, we predicted potential N-linked glycosylation sites at asparagines 56, 379, 401, and 438 of the IHNV G protein using the NetNGlyc 1.0 Server, constructed nine recombinant IHNVs with either single or multiple mutations of the predicted glycosylation sites, and evaluated their respective contributions to viral pathogenicity and immunogenicity.

2. Materials and methods

All applicable international and national guidelines for the care and use of animals were followed. The animal protocol for this research was approved by the Animal Care and Use Committee of Northeast Agricultural University, China.

2.1. Viruses, cells, and animals

Wild-type IHNV (wtIHNV) HLJ-09 (GenBank accession number JX649101) was isolated by, and stored in our laboratory. Recombinant IHNV (rIHNV) HLJ-09 was constructed in our laboratory [25]. Epithelioma papulosum cyprinid (EPC) cells, Chinook salmon embryo (CHSE-214) cells, and rainbow trout gonad (RTG-2) cells (ATCC, USA) were cultured in Leibovitz's L-15 medium supplemented with 10% fetal bovine serum (FBS) (Gibco, USA) at 16 °C. Healthy juvenile rainbow trout weighing approximately either 1 g or 10 g were obtained from the Bohai Cold Water Fish Experimental Station, China, and kept in 120 cm × 50 cm × 60 cm tanks at 16 °C for two weeks to adapt to the environment. Moreover, in this study, all the viruses used for *in vivo* or *in vitro* experiments were subjected to being sequenced targeting the G gene to confirm the presence of the targeted mutation and the absence of other mutations in the G gene.

2.2. Plasmids, antibodies, and primers

Recombinant plasmid pBlueScript II SK-F543216 containing full-length IHNV HLJ-09 cDNA, and plasmids pCI-IHNV-HLJ-09, pCI-G, pCI-N, pCI-P, pCI-L, pCI-NV, pMD18-T-F2, and pMD18-T-F3 (F2 and F3 segments are shown in Fig. 1B) were constructed in our laboratory [25]. Rabbit anti-IHNV G protein serum antibody, rabbit anti-rainbow trout IgM serum antibody, and mouse anti-IHNV serum antibody were prepared in our laboratory. All primers used in this work are listed in Table 1.

2.3. Prediction of glycosylation sites in the IHNV G protein

IHNV G protein glycosylation sites were predicted using the NetNGlyc 1.0 Server at http://www.cbs.dtu.dk/services/NetNGlyc/, which predicted four possible N-linked asparagine (Asp, N) glycosylation sites at amino acid positions 56, 379, 401, and 438 (Fig. 1A).

2.4. Construction of recombinant full-length cDNA of IHNV

Recombinant full-length cDNAs of IHNV HLJ-09 with single or multiple alanine substitutions at predicted G protein glycosylation sites were constructed according to the schematic shown in Fig. 1B, using the recombinant plasmids described in Section 2.2 as templates. In brief, the corresponding sites at position of asparagines 56, 379, 401, and 438 in IHNV G protein were mutated with single site, triple sites, or quadruple sites on F2 and F3 segments by overlapping PCR assay, respectively; and then, F2 and F3 segments in intermediate vector pBlueScript II SK-F543216 were replaced by the F2 and F3 segments with site-directed mutations, respectively; subsequently, the full-length cDNA in pBlueScript II SK-F543216 was digested and subcloned into the eukaryotic plasmid pCI, yielding nine recombinant plasmids pCI-N56A, pCI-N379A, pCI-N401A, pCI-N438A, pCI-N56A-N379A-N401A, pCI-N56A-N379A-N438A, pCI-N56A-N401A-N438A, pCI-N379A-N401A-N438A, and pCI-N56A-N379A-N401A-N438A.

Table 1
Primers used in this study.

Primers	Sequences (5′–3′)	Position[a] (bp)
IHNV SnaBF[b]	CTAAAA*TACGTA*GAGGAGGAG	1696–1676
IHNV SpeR[b]	TGCATGGAG*ACTAGT*GGAGTC	5244–5220
IHNV NdeR	TGTGGTGT*CATATG*CCCCTGC	3414–3390
IHNV NdeF	GCAGGGG*CATATG*ACACCACA	3412–3392
IHNV-G-N56AF	TCCAAGGTC*GCT*GCTTCTCAA	3155–3175
IHNV-G-N56AR	TTGAGAAGCA*GC*GACCTTGGA	3175–3155
IHNV-G-N379AF	ATCACGCCACC*GCC*TTCACTA	4122–4142
IHNV-G-N379AR	TAGTGAA*GC*GGTGGCGTGAT	4142–4122
IHNV-G-N401AF	CACGGAAAC*GCC*ATCACCATT	4190–4210
IHNV-G-N401AR	AATGGTGAT*GC*GTTTCCGTG	4210–4190
IHNV-G-N438AF	GCCTTCTAC*GCT*GAGACAGAA	4301–4321
IHNV-G-N438AR	TTCTGTCTCA*GC*GTAGAAGGC	4321–4301
IHNV-G-KpnF	*GGTACC*GCCACCATGGACGCCATGATCA	2999–3014
IHNV-G-SalR	*GTCGAC*TTAGGACCTGTTTGCC	4525–4510
IHNV RTFQ-F	TCTTCAGATAGAGTTCGTGGAGGG	5490–5513
IHNV RTFQ-R	CGCATACGGTGTTACACTTGGGAG	5595–5572

[a] The reference strain was IHNV HLJ-09 (GenBank Accession No. JX649101).
[b] Which represents synonymous mutation; The italics represents digestion sites; The underline represent mutated bases.

2.5. Recovery of recombinant IHNVs

CHSE-214 cells were grown to 80–90% confluence in 24-well plates with Leibovitz's L-15 medium supplemented with 10% FBS (Gibco, USA) at 16 °C. Prior to transfection, 0.5 μg of each recombinant G protein plasmid was mixed with the five helper plasmids required for RNA encapsidation and replication (0.25 μg pCI-N, 0.25 μg pCI-P, 0.1 μg pCI-L, 0.05 μg pCI-NV, and 0.05 μg pCI-G) in 100 μL FBS-free Leibovitz's L-15 medium, and transfected into CHSE-214 cells using Lipofectamine LTX and PLUS™ Reagents (Invitrogen, USA) according to the manufacturer's instructions. Transfection with empty pCI, transfection reagents alone, and mock CHSE-214 cells were used as controls. After transfection, cells were incubated in a 5% CO_2 incubator at 16 °C for 7 days followed by observation of virus-induced cytopathic effects (CPEs); identification by RT-PCR with primers IHNV-G-KpnF/IHNV-G-SalR; and after three passages with monitoring of CPEs, nine recombinant viruses rIHNV-N56A, rIHNV-N379A, rIHNV-N401A, rIHNV-N438A, rIHNV-N56A-N379A-N401A, rIHNV-N56A-N379A-N438A, rIHNV-N56A-N401A-N438A, rIHNV-N379A-N401A-N438A, and rIHNV-N56A-N379A-N401A-N438A were recovered. Details of amino acid replacement locations in these recombinant viruses are shown in Table 2.

2.6. Identification of recombinant IHNVs

Indirect immunofluorescence assay (IFA) and transmission electron microscopy (TEM) assays were used to confirm recovery of recombinant IHNVs. For identification using IFA, each recombinant IHNV was passaged five times before inoculation onto a CHSE-214 cell monolayer grown to approximately 50% confluence in a 24-well plate, and incubated at 16 °C for 36 h. Cells were next washed twice with sterile PBS, fixed with 4% paraformaldehyde for 15 min, and permeabilized with 0.2% Triton X-100 for 10 min. Subsequently, cells were blocked with 0.3% bovine serum albumin (BSA) at 37 °C for 30 min, incubated with mouse anti-IHNV serum primary antibodies (prepared by our lab) and fluorescein isothiocyanate (FITC)-conjugated goat anti-mouse IgG secondary antibodies (Thermo Fisher Scientific Inc., USA), and visualized

Table 2
Details of N-glycosylated asparagine replacement locations in recombinant viral genomes.

Recombinant viruses	G-N56A AAT→GCT	G-N379A AAC→GCC	G-N401A AAC→GCC	G-N438A AAT→GCT
rIHNV- N56A	✓	–	–	–
rIHNV-N379A	–	✓	–	–
rIHNV-N401A	–	–	✓	–
rIHNV-N438A	–	–	–	✓
rIHNV-N56A-N379A-N401A	✓	✓	✓	–
rIHNV-N56A-N379A-N438A	✓	✓	–	✓
rIHNV- N56A-N401A-N438A	✓	–	✓	✓
rIHNV- N379A-N401A-N438A	–	✓	✓	✓
rIHNV-N56A-N379A-N401A-N438A	✓	✓	✓	✓
rIHNV HLJ-09	–	–	–	–

by immunofluorescence using an Axio Observer A1 fluorescence microscope (ZEISS, Germany). For TEM imaging, each recombinant IHNV was passaged five times before inoculation onto a CHSE-214 cell monolayer and incubated at 16 °C for 60 h, for evaluation of CPE. Samples were prepared for TEM by fixation, dehydration, embedding and polymerization, ultrathin slice preparation, and staining with lead citrate and uranyl acetate; viral morphology was visualized using an H-7650 transmission electron microscope (Hitachi Limited, Japan).

2.7. Determining the effect of disrupting IHNV G protein glycosylation

Recombinant IHNVs with mutated G protein glycosylation sites were passaged five times, propagated on CHSE-214 cell monolayers, and incubated at 16 °C for 60 h. Subsequently, culture supernatants were collected, centrifuged, 20 × concentrated by PEG 8000 (Sigma, USA) precipitation, mixed with 5 × sodium dodecyl sulfate (SDS) loading buffer, and denatured in boiling water for 10 min for analysis by 12% SDS-polyacrylamide gel electrophoresis (SDS-PAGE). After SDS-PAGE, the proteins were transferred onto a polyvinylidene fluoride membrane, and immunoblots developed using rabbit anti-IHNV G protein serum (prepared by our lab) as the primary antibody and horseradish peroxidase (HRP)-conjugated goat anti-rabbit antibody (Thermo Fisher Scientific Inc., USA), as the secondary antibody, using wtIHNV HLJ-09 strain as a control. In parallel, concentrated culture supernatants from each recombinant IHNV were treated with Peptide-N-Glycosidase F (PNGase F) (NEB, USA) at 37 °C for 1 h, before analysis by western blotting as described above.

2.8. Determination of recombinant IHNV growth curves and cell tropism

CHSE-214 cell monolayers grown at 16 °C in Leibovitz's L-15 medium supplemented with 10% FBS (Gibco, USA) were inoculated with 100 $TCID_{50}$ of each recombinant IHNV and cultured at 16 °C; cell cultures were collected 24, 36, 48, 60, 72, 84, and 96 h post-inoculation, and virus titers (Log10 $TCID_{50}$/mL) calculated using the Reed-Muench method. Cell tropisms of recombinant IHNVs were evaluated by inoculating 100 $TCID_{50}$ of wtIHNV HLJ-09 and the nine recombinant IHNV strains onto EPC, CHSE-214, and RTG-2 cell monolayers, respectively cultured at 16 °C for 72 h, and virus titers (Log10 $TCID_{50}$/mL) were calculated by the Reed-Muench method.

2.9. Measurement of recombinant IHNV pathogenicity and in vivo growth

Juvenile rainbow trout of mean weight ~1 g were randomly assorted into 12 groups of 40 fish each. Fish from groups 1 to 11 were injected with 50 μL (approximately 10^5 $TCID_{50}$/mL) of rIHNV HLJ-09 strain, rIHNV-N56A, rIHNV-N379A, rIHNV-N401A, rIHNV-N438A, rIHNV-N56A-N379A-N401A, rIHNV-N56A-N379A-N438A, rIHNV-N56A-N401A-N438A, rIHNV-N379A-N401A-N438A, rIHNV-N56A-N379A-N401A-N438A, and wtIHNV HLJ-09 strain recovered after passaging nine times, respectively; fish from group 12 were injected with PBS as a mock-infection negative control. In parallel, another 11 groups of 40 fish each were respectively infected by bath immersion with equivalent dose of viruses, and the group of fish immersed with PBS was used as a mock-infection negative control. The 30-day cumulative mortality of fish in each group was recorded, and the liver, kidney, and heart samples of fish were inspected for histopathological changes, at the same time, the recombinant viruses recovered from dead fish were subjected to being sequenced targeting the G gene in order to detect any reversion events in fish. Moreover, active replication of recombinant IHNVs in rainbow trout was detected using a SYBR Green-based quantitative real-time RT-PCR (RT-qPCR) assay. In brief, juvenile rainbow trout of mean weight ~10 g were randomly assorted into 11 groups of five fish each, and fish from groups 1 to 10 were injected with 100 μL 10^5 $TCID_{50}$/mL of either wtIHNV HLJ-09 or one of the nine recombinant viruses as described above, and fish from group 11 were injected with PBS as a mock-infection negative control. In parallel, another 10 groups of five fish each were respectively infected by bath immersion with equivalent dose of viruses, and the group of fish immersed with PBS was used as a mock-infection negative control. After 72 h, viral genome copy numbers in fish kidney and liver samples were quantified by RT-qPCR using IHNV RTFQ-F and IHNV RTFQ-R primers. In order to calculate viral genome copy numbers, the plasmid pBlueScript II SK-F543216 containing the full-length cDNA of IHNV was used as a standard to establish the standard curve for the RT-qPCR assay. The standard curve formula was: $Y = -3.253X + 32.781$, $R^2 = 0.997$.

2.10. Determination of specific anti-IHNV IgM immune response by rainbow trout

To detect the fish immune response induced by infection with recombinant rIHNVs, specific IgM antibody levels were detected using an indirect ELISA assay. Briefly, juvenile rainbow trout of mean weight ~10 g were randomly assorted into 11 groups of 15 fish each, and fish from groups 1 to 10 injected with either 50 μL 10^5 $TCID_{50}$/mL wtIHNV HLJ-09 or one of the nine recombinant viruses, and fish in group 11 injected with L-15 medium as a mock-infection negative control (for this experiment, it is difficult for a single fish weighing 10 g to live to get enough serum samples for detection, so we have to harvest the serum from all 15 fish per group at each time point, which was used to evaluate the IgM titration, thus each fish can still survive). On days 14, 28, 42 and 56 post-infection, approximately 50 μL serum samples were collected from each group for anti-IHNV IgM antibody detection by ELISA. A 96-well ELISA plate was coated with 200 μL wtIHNV HLJ-09, incubated at 4 °C overnight, blocked with 200 μL 5% skimmed milk at 37 °C for 2 h, then incubated at 37 °C for 1 h using rainbow trout sera diluted 1:32 as the primary antibody, and HRP-conjugated rabbit anti-rainbow trout IgM diluted 1:1000 (prepared by our laboratory) as the secondary antibody. Binding was quantified by measurement of color change of the tetramethylbenzidine (TMB) (Qiagen, Germany) reaction catalyzed by HRP, measured at a wavelength of 450 nm.

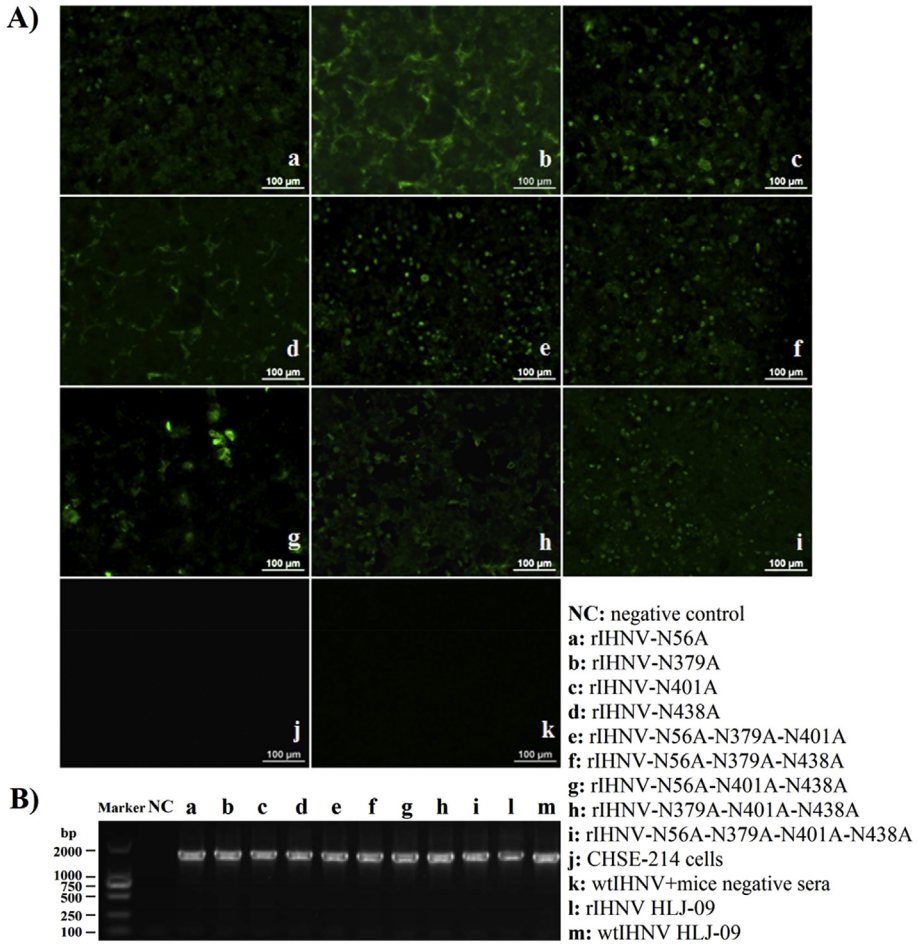

Fig. 2. Confirmation of recombinant viruses by indirect immunofluorescence assay (IFA), and identification of recombinant viruses by RT-PCR. A): The nine recombinant infectious hematopoietic necrosis viruses (rIHNVs) were propagated on CHSE-214 cell monolayers at 16 °C for 36 h, followed by fixation with 4% paraformaldehyde for 15 min, and permeabilization with 0.2% Triton X-100 for 10 min. After blocking with 0.3% bovine serum albumin, immunofluorescence was developed using mouse anti-IHNV sera as the primary antibody and FITC-conjugated goat anti-mouse IgG as the secondary antibody, and observed by fluorescence microscopy. B): RT-PCR confirms presence of recombinant viruses by amplification of PCR products consistent with the predicted size. a: rIHNV-N56A; b: rIHNV-N379A; c: rIHNV-N401A; d: rIHNV-N438A; e: rIHNV-N56A-N379A-N401A; f: rIHNV-N56A-N379A-N438A; g: rIHNV-N56A-N401A-N438A; h: rIHNV-N379A-N401A-N438A; i: rIHNV-N56A-N379A-N401A-N438A; j: CHSE-214 cells negative control; k: wild-type IHNV using mouse negative sera control; l: rIHNV HLJ-09; m: wild-type IHNV.

2.11. Statistical analysis

All experiments were performed with at least three replicates, and data are shown as mean ± standard error. Student's t-test was used to determine statistical significance. $P < 0.05$ was considered a significant difference, while $P < 0.01$ was considered a highly significant difference.

3. Results

3.1. Identification by recombinant viruses

Seven days after transfection of CHSE-214 cells with plasmids encoding rIHNV with glycosylation-disrupted G proteins, we clearly observed virus-induced CPEs comparable to those induced by both rIHNV HLJ-09 and wtIHNV HLJ-09 (data not shown), while no CPEs were observed in our negative controls. These recombinant viruses can be specifically recognized by mouse anti-IHNV sera in an IFA assay (Fig. 2A: a-i), while no specific fluorescence was observed in the CHSE-214 cell negative control (Fig. 2A: j) or wtIHNV using mouse negative sera control (Fig. 2A: k). Moreover, to confirm the identity of the recombinant viruses, we purified viral genomic RNA and used an RT-PCR assay to confirm that a specific band amplified from each virus consistent with the predicted size of 1530 bp (Fig. 2B). We also used TEM to image recombinant viruses that had been propagated on CHSE-214 cells for five passages, and our TEM results confirmed that each recombinant virus produced virions that matched the typical 160 nm × 80 nm bullet shape of IHNV (Fig. 3). Therefore, based on the results above, we concluded that the recombinant viruses had been constructed successfully.

3.2. Detection of G protein glycosylation of recombinant viruses

To confirm patterns of G protein glycosylation in the nine recombinant IHNVs, we concentrated supernatant from CHSE-214 cells that had been inoculated with each rIHNV strain for G protein Western blot analysis, and compared our results with western blots of the same supernatant after N-glycosyl cleavage. As shown in Fig. 4A, a ~70 kDa immunoblot band was observed in wtIHNV HLJ-09 (lane 1); a ~67 kDa band was observed in rIHNV-N56A, rIHNV-N379A, rIHNV-N401A, and rIHNV-N438A (lanes 2 to 5, respectively); a ~59 kDa band was observed in rIHNV-N56A-N379A-N401A, rIHNV-N56A-N379A-N438A, rIHNV-N56A-N401A-N438A, and rIHNV-N379A-N401A-N438A (lanes 6 to 9 respectively); and a ~55 kDa band was observed in rIHNV-N56A-N379A-N401A-N438A (lane 10). These molecular weight differences between samples were consistent with disruption of zero, one, three, or four N-glycosylation sites for the samples loaded in lane 1 (wtIHNV), lanes 2 to 5 (single point mutants), lanes 6 to 9 (triple point mutants), and lane 10 (a quadruple point mutant), respectively. To further confirm that these molecular weight differences were due to N-glycosylation alone, culture supernatant from each recombinant IHNV was treated with PNGase F and analyzed again by Western blot, demonstrating that wtIHNV HLJ-09 and all nine recombinant IHNVs produce similar ~55 kDa band (Fig. 4B), consistent with the core protein from the rIHNV-N56A-N379A-N401A-N438A (Fig. 4A: lane 10) being the same molecular weight. Based on these results, we could conclude that the asparagines at positions 56, 379, 401, and 438 of the IHNV G protein are N-linked glycosylation sites, and the quality of the oligosaccharides present in all four glycosylation sites is similar.

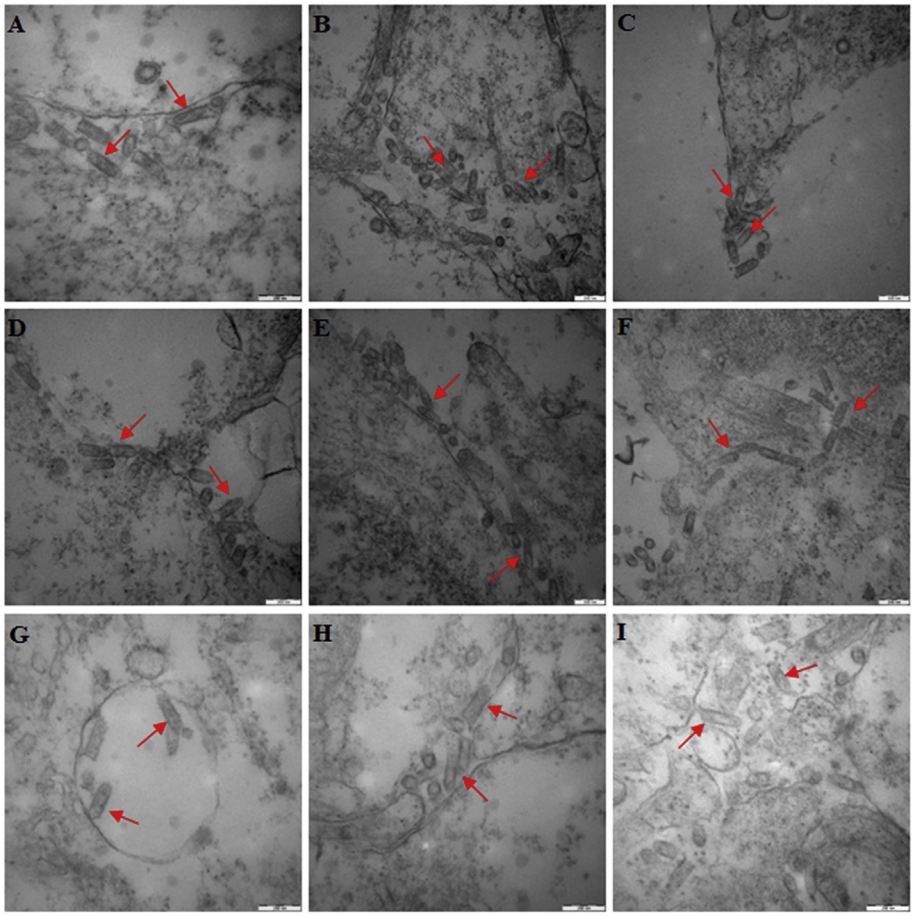

Fig. 3. Transmission electron microscopy (TEM) confirms the presence of infectious hematopoietic necrosis virus (IHNV) virion-like structures after transfection. Following fixation, dehydration, embedding and polymerization, ultrathin slice preparation, and staining with lead citrate and uranyl acetate, recombinant viruses were imaged by TEM, demonstrating that each recombinant virus produces 160 nm × 80 nm bullet-shaped virions typical of IHNV. A: rIHNV-N56A; B: rIHNV-N379A; C: rIHNV-N401A; D: rIHNV-N438A; E: rIHNV-N56A-N379A-N401A; F: rIHNV-N56A-N379A-N438A; G: rIHNV-N56A-N401A-N438A; H: rIHNV-N379A-N401A-N438A; I: rIHNV-N56A-N379A-N401A-N438A.

3.3. Growth curves and cell tropisms of recombinant IHNVs

To determine viral growth curves, we propagated wtIHNV HLJ-09 and the nine recombinant viruses on CHSE-214 cells. As shown in Fig. 5A, viral titers of the nine recombinant IHNVs at the plateau phase were lower than that of wtIHNV HLJ-09; notably, the viral titers of rIHNV-N56A-N401A-N438A, rIHNV-N379A-N401A-N438A, and rIHNV-N56A-N379A-N401A-N438A were significantly lower than wtIHNV, indicating that single or combined mutation of IHNV G protein glycosylation sites impaired the replication ability of recombinant viruses, particularly mutants that combined disruption of the asparagines at positions 401 and 438. Moreover, we found that the cell tropisms of the nine recombinant viruses were comparable to wtIHNV as determined by comparing viral titers in CHSE-214, EPC, and RTG-2 cells 72 h post-infection (Fig. 5B). Of which the titers of all viruses were significantly higher in EPC and CHSE-214 cells than those of RTG-2 cells; the titers of rIHNV-N56A-N401A-N438A, rIHNV-N379A-N401A-N438A, and rIHNV-N56A-N379A-N401A-N438A were significantly lower ($p < 0.05$) than those of other recombinant IHNVs in all three cells types.

3.4. Pathogenicity of recombinant IHNVs

We sought to evaluate the virulence implications of disrupting G protein N-glycosylation by challenging fish with the nine recombinant IHNVs by injection or bath immersion and comparing cumulative mortality in each group over 30 days. Our results showed that whether being infected by injection (Fig. 6A) or bath immersion (Fig. 6B), the cumulative mortality of fish infected with rIHNV-N56A, rIHNV-N379A, rIHNV-N401A, rIHNV-N56A-N379A-N401A, rIHNV-N56A-N401A-N438A, rIHNV-N379A-N401A-N438A, and rIHNV-N56A-N379A-N401A-N438A was nearly 100%, and the cumulative mortality of fish infected with rIHNV-N56A-N379A-N438A by injection (Fig. 6A) and by bath immersion (Fig. 6B) was approximately 95% and 92.5%,

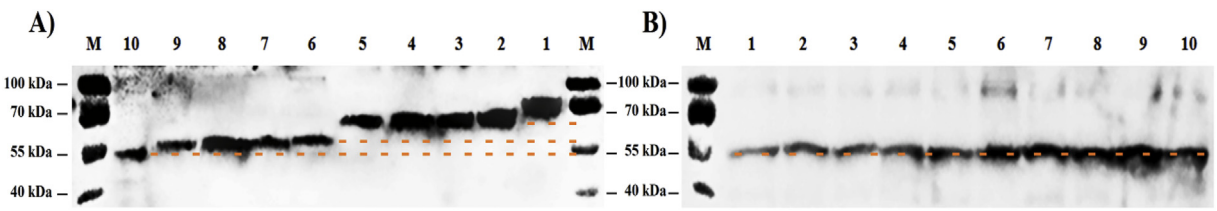

Fig. 4. Western blot analysis of predicted G protein glycosylation site mutants and proteins after N-glycan cleavage confirmed four glycosylation sites in wild-type IHNV and their successful disruption in nine recombinant mutants (rIHNV). Culture supernatant of rIHNVs that was treated without Peptide-N-Glycosidase F (PNGase F) (A) and with PNGase F (B) was analyzed by Western blot. Lanes: 1, wtIHNV; 2, rIHNV-N56A; 3, rIHNV-N379A; 4, rIHNV-N401A; 5, rIHNV-N438A; 6, rIHNV-N56A-N379A-N401A; 7, rIHNV-N56A-N379A-N438A; 8, rIHNV-N56A-N401A-N438A; 9, rIHNV-N379A-N401A-N438A; 10, rIHNV-N56A-N379A-N401A-N438A; M, protein marker.

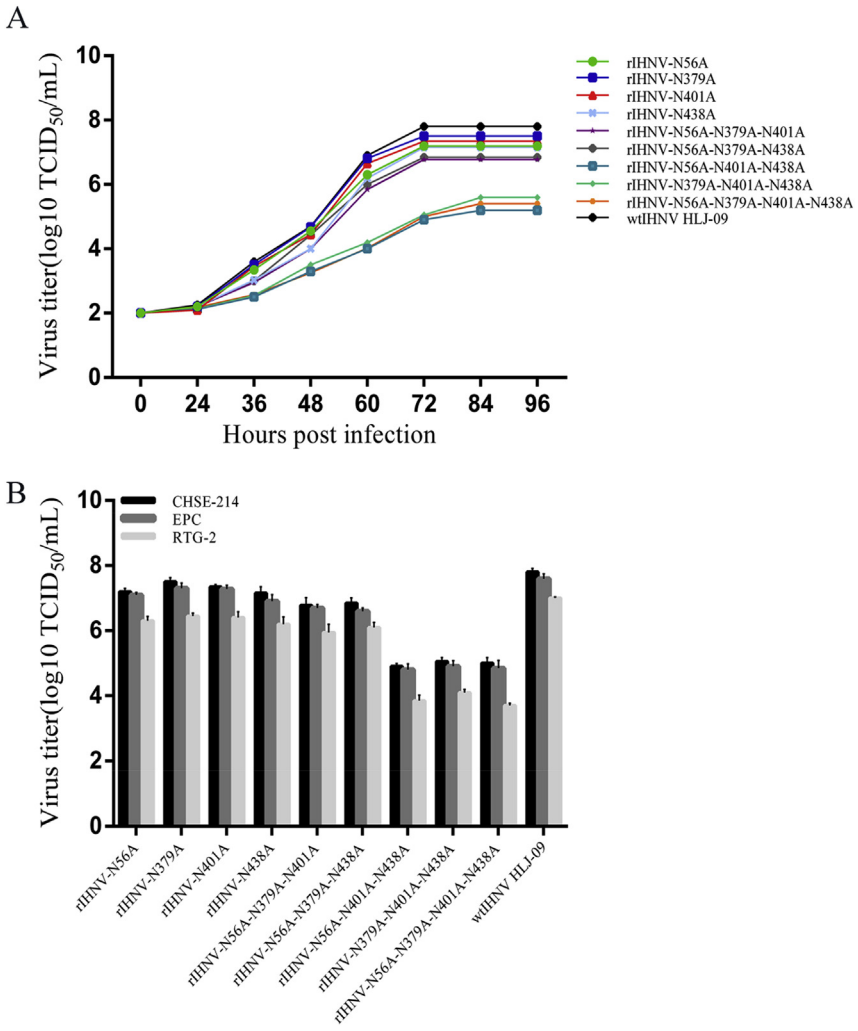

Fig. 5. Growth curves of recombinant viruses in CHSE-214 cells (A) and cell tropisms of wild-type and recombinant viruses (B). Viral titers for all strains were significantly higher in EPC and CHSE-214 cells than those in RTG-2 cells, while the viral titers of rIHNV-N56A-N401A-N438A, rIHNV-N379A-N401A-N438A, and rIHNV-N56A-N379A-N401A-N438A in CHSE-214, EPC, and RTG-2 cells were significantly lower ($p < 0.05$) than those of other recombinant IHNVs.

respectively. Significantly, the cumulative mortality of fish infected with rIHNV-N438A was only 47.5% by injection (Figs. 6A) and 42% by bath immersion (Fig. 6B), indicating that mutation of asparagine 438 alone significantly reduces the pathogenicity of this strain.

Moreover, we observed histopathological changes in the livers, kidneys, and hearts of each group. As shown in Fig. 7, the livers of fish challenged with rIHNV-N56A, rIHNV-N379A, rIHNV-N401A, rIHNV-N56A-N379A-N401A, and rIHNV-N56A-N379A-N438A showed significant degeneration of hepatocytes, nuclear lysis, incomplete cell membranes, balloon-like degeneration and necrosis in some cells, and whole or partial disappearance of hepatic cord structure with proliferated interstitial components. Renal lesions of fish in these groups were characterized mainly by tissue necrosis, granular lesions and swelling of cells in the necrotic area, renal tubular necrosis, and swelling and vacuolar degeneration of proximal convoluted tubular epithelial cells. The most prominent manifestations of cardiac pathological lesions of fish in rIHNV-N56A, rIHNV-N379A, rIHNV-N401A, rIHNV-N56A-N379A-N401A, and rIHNV-N56A-N379A-N438A groups were disordered arrangement of cardiac myocytes, light staining of nuclei, and transverse interstitial enlargement. Some pathological changes of the liver, kidney and heart of fish challenged with rIHNV-N438A, rIHNV-N56A-N379A-N438A, rIHNV-N56A-N401A-N438A, rIHNV-N379A-N401A-N438A, and rIHNV-N56A-N379A-N401A-N438A were observed. Of which the degrees of liver, kidney, and heart lesions of fish in the rIHNV-N438A group were relatively mild. From the results above, we concluded that the difference in pathological changes reflected the difference in the pathogenicity of recombinant viruses. We also performed sequencing analysis targeting the G gene of each recombinant virus recovered from dead fish, and our data showed that there was no reversion events observed in fish. Moreover, we determined genome copy numbers of recombinant viruses in livers and kidneys of fish using RT-qPCR, and found that whether being infected with the nine recombinant IHNVs by injection or bath immersion, the viral genome copy numbers in liver (Fig. 8A) and kidney (Fig. 8B) of fish were lower than those in liver and kidney of fish infected with wtIHNV HLJ-09 strain, consistent with our earlier observations, suggesting that mutation of glycosylation sites in the IHNV G protein impairs viral replication *in vivo*.

3.5. Specific anti-IHNV IgM levels in fish infected with recombinant IHNVs

To assess fish immune responses to recombinant IHNVs, we collected serum samples from the eleven rainbow trout groups on days 14, 28, 42, and 56 post-challenge with each rIHNV, and measured titers of specific anti-IHNV IgM antibodies by indirect ELISA assay. As shown in Fig. 8C, all nine recombinant viruses induced production of specific anti-IHNV IgM antibodies. Of which significant levels ($p < 0.05$) of IgM antibody were induced by recombinant viruses on days 28 post-

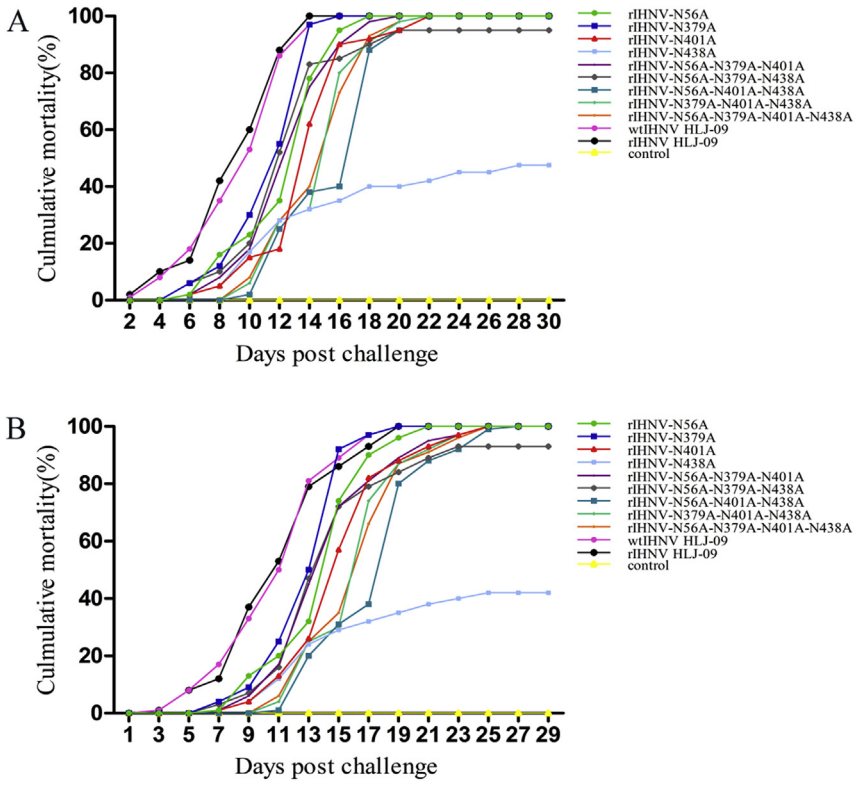

Fig. 6. Cumulative mortality of rainbow trout challenged with recombinant viruses by injection (A) and by bath immersion (B). Juvenile rainbow trout weighing ~1 g were challenged with 50 μL 10^5 $TCID_{50}$ of wtIHNV HLJ-09, rIHNV HLJ-09, rIHNV-N56A, rIHNV-N379A, rIHNV-N401A, rIHNV-N438A, rIHNV-N56A-N379A-N401A, rIHNV-N56A-N379A-N438A, rIHNV-N56A-N401A-N438A, rIHNV-N379A-N401A-N438A, and rIHNV-N56A-N379A-N401A-N438A by injection and by bath immersion, and thirty-day cumulative mortality of each group was recorded.

challenge, particularly the rIHNV-N438A, which could induce significant level ($p < 0.05$) of IgM antibody production earlier. We subsequently assessed the IHNV immunoprotection conferred to those rainbow trout challenged with rIHNV-N438A, finding a 75% survival rate, demonstrating substantial immunoprotection conferred by rIHNV-N438A challenge (Fig. 8D).

4. Discussion

The worldwide spread of IHNV has seriously restricted the development of the aquaculture industry, especially salmon farming. Although there are many reports about the development of vaccines against IHNV, including inactivated virus vaccines [26], attenuated vaccines [27], and DNA vaccines [28,29], most are still at the research

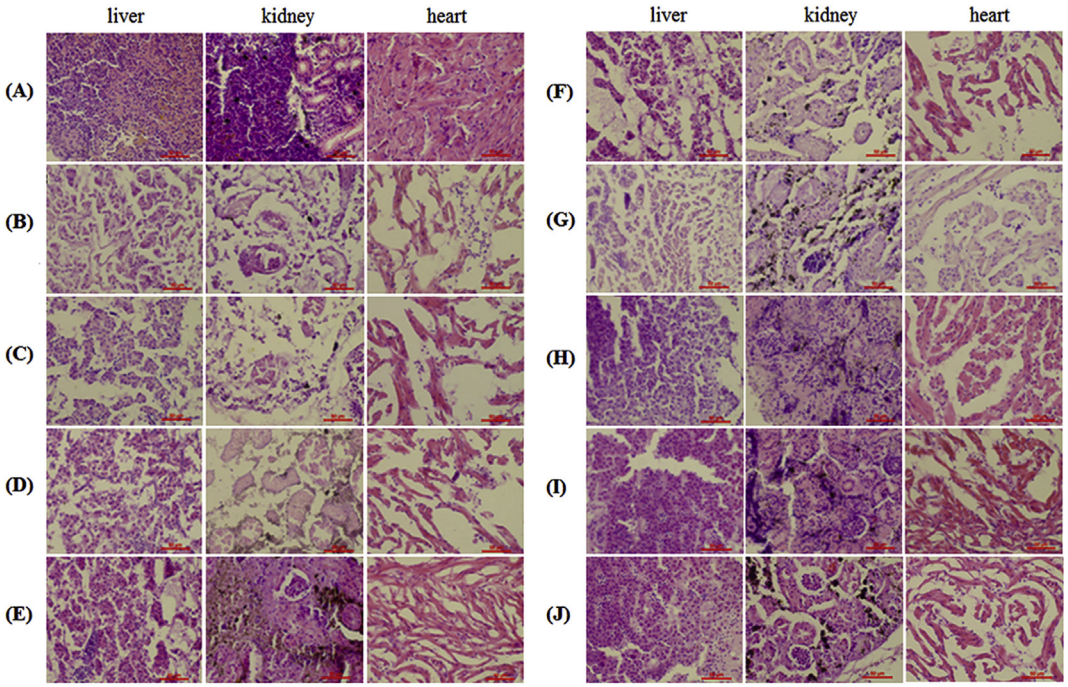

Fig. 7. Histopathological changes in fish infected with recombinant infectious hematopoietic necrosis viruses (rIHNVs) (400×). (A) Normal control; (B) rIHNV-N56A; (C) rIHNV-N379A; (D) rIHNV-N401A; (E) rIHNV-N438A; (F) rIHNV-N56A-N379A-N401A; (G) rIHNV-N56A-N379A-N438A; (H) rIHNV-N56A-N401A-N438A; (I) rIHNV-N379A-N401A-N438A; (J) rIHNV-N56A-N379A-N401A-N438A.

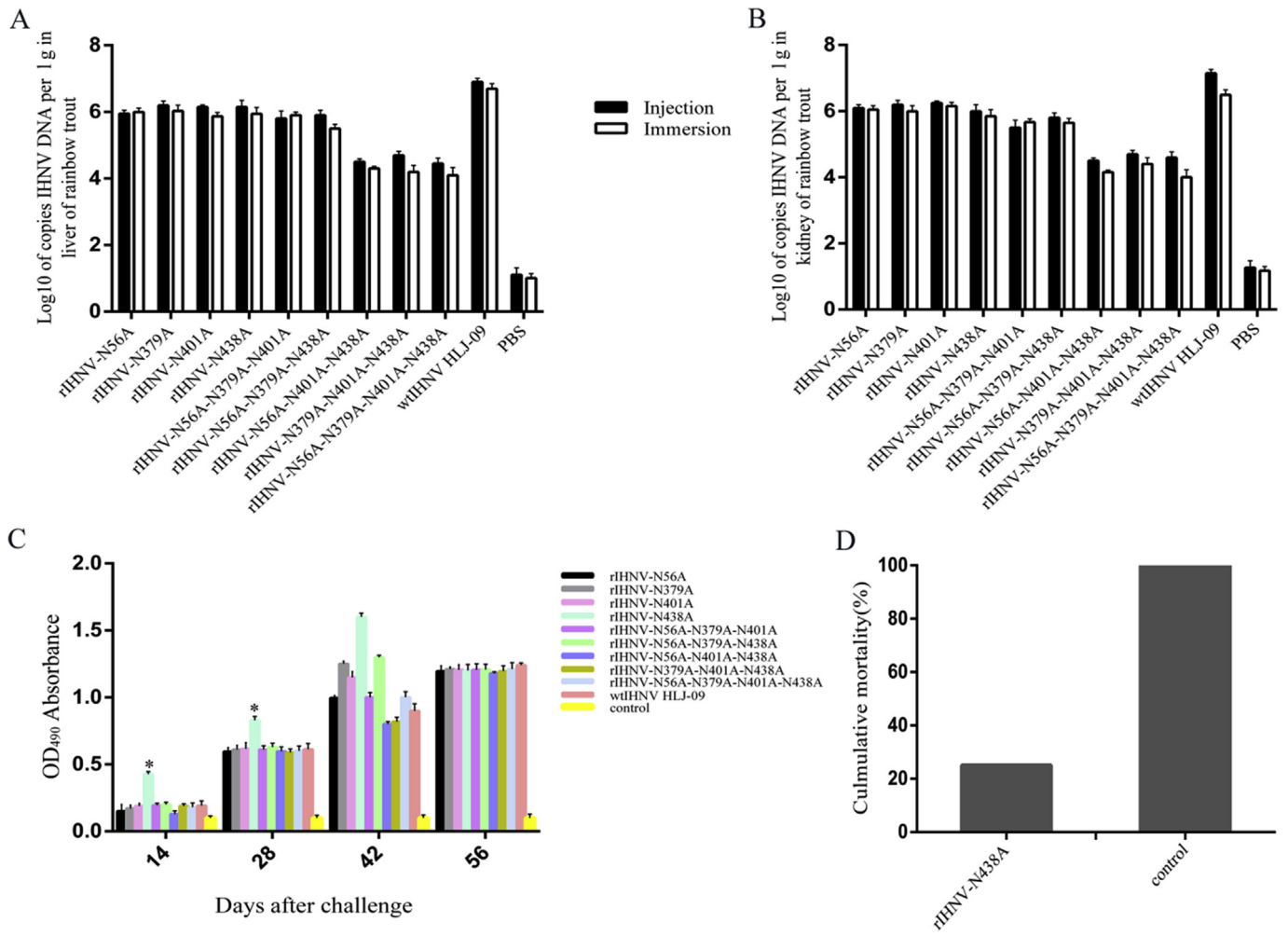

Fig. 8. Replication is impaired in recombinant viruses. The active replication ability of each recombinant infectious hematopoietic necrosis virus (rIHNV) in rainbow trout liver (A) and kidney (B) after infection with 100 μL 10^5 $TCID_{50}$/mL recombinant viruses by injection or bath immersion, followed by RT-qPCR quantification of genome copy numbers 72 h post-infection. (C) IgM levels in serum from rainbow trout of mean weight ~10 g challenged with 50 μL 10^5 $TCID_{50}$/mL recombinant viruses were measured by ELISA 14, 28, 42, and 56 days post-infection. (D) Thirty-day cumulative mortality of fish vaccinated with rIHNV-N438A prior to challenge with wild-type IHNV HLJ-09.

laboratory stage of development. Although the immunogenicity of traditional attenuated vaccines is superior to other types of vaccines, because different fish species have different viral susceptibilities, an attenuated vaccine that is effective for one species may be pathogenic to another. Furthermore, a risk inherent to attenuated vaccines is the possibility of their reversion to virulence. Thankfully, the development of reverse genetics technology makes it possible to obtain safe and effective attenuated vaccines by knocking out or mutating virulence sites or pathogenic genes [30–32].

Reverse genetic techniques play an increasingly important role in RNA virus research. Using reverse genetics, we can use point mutations, gene insertions or knockouts, gene replacements, or gene recombination to investigate the relationship between protein structure and function, and the mechanisms of viral pathogenesis [33]. Studies have indicated that envelope protein glycosylation may directly affect the virulence, replication ability, and immunogenicity of viruses [17,18,24]. The IHNV G protein is an envelope protein that plays an important role in virulence and pathogenic mechanism of IHNV [5,29]. In this study, in order to explore the effects of IHNV G protein glycosylation on virulence, replication ability, and immunogenicity, we identified four potential glycosylation sites at asparagines 56, 379, 401, and 438, and constructed nine recombinant viruses with different combinations of single or multiple asparagine-to-alanine substitutions at these sites. These mutants had single, triple, or quadruple glycosylation site point mutations that we confirmed using RT-PCR, TEM, and IFA assays. Subsequently, Western blot analysis further confirmed the presence of the four predicted glycosylation sites, and these sites mutation could reduce glycosylation of G protein of the nine rIHNVs. Moreover, from the results of Western blot for the culture supernatant of rIHNVs (with single, triple, or quadruple glycosylation site point mutations) without Peptide-N-Glycosidase F treatment, we could conclude that the quality of the oligosaccharides present in all four glycosylation sites at positions 56, 379, 401, and 438 of the IHNV G protein is similar.

For many enveloped viruses such as tick-borne encephalitis virus and Hantaan virus, glycosylation of envelope protein achieved by adding glycosyl groups plays important role in viral invasion and replication [20,34], impairing envelope protein glycosylation could affect viral cell entry, and the assembly and secretion of viral particles [34]. We analyzed the replication ability of the nine recombinant IHNVs *in vitro* and *in vivo*, finding that the replication ability of these recombinant viruses was lower than that of wtIHNV. Moreover, the difference in replication ability between recombinant viruses and wild-type virus was not attributable to host cell type, indicating that the mutation of G protein glycosylation sites specifically affects viral replication ability, and not cell entry. Notably, the replication ability of

recombinant viruses with combined mutations of asparagines 401 and 438 reduced significantly. Similarly, mutation of the glycosylation site at amino acid 116 of the swine fever virus E2 glycoprotein significantly reduces replication ability of the virus [17]. It is speculated that glycosylation impairment may alter the conformation of the envelope protein, thus slowing replication in host cells. The mechanisms underlying this, however, remain to be identified.

Previous studies have demonstrated that glycosylation of viral outer membrane proteins may mask viral antigenic epitopes, preventing the host from producing antibodies, and resulting in virus immune escape that enables continued infection [22–24]. Impairing glycosylation, however, avoids this problem, and could effectively both reduce viral replication ability and virulence, and enhance viral immunogenicity [15,16]. In this study, we found that anti-IHNV IgM levels induced by challenge with rIHNV-N438A, which has only a single N438A mutation, increased quicker, and by more, than those induced by the other recombinant viruses, indicating that the humoral immune response of rainbow trout to IHNV was enhanced when exposed to rIHNV-N438A. Similarly, mutation of a glycosylation site on the GP5 protein from porcine reproductive and respiratory syndrome virus also induces high antibody levels in mice [24]. We speculate that amino acid 438 of the IHNV G protein may be related to immune escape, because it is located in the neutralizing epitope area between amino acids 419 to 444 [13,14]. Indeed, the conformational change in the G protein with a single point mutation at asparagine 438 may differ from that of combined mutation of asparagines 56, 379, 401, and 438, affecting exposure of the neutralization epitope differently, and inducing different fish IgM antibody levels. The virulence of the recombinant IHNVs was also directly affected by the impairment of glycosylation of the G protein. Although the 30-day cumulative mortality rates of rainbow trout infected with rIHNV-N56A, rIHNV-N379A, rIHNV-N401A, rIHNV-N56A-N379A-N401A, rIHNV-N56A-N401A-N438A, rIHNV-N379A-N401A-N438A, and rIHNV-N56A-N379A-N401A-N438A were the same as those infected with wtIHNV, their death time was substantially delayed. Significantly, the mortality rate of fish in the rIHNV-N438A group has fallen dramatically, because there was no significant difference in growth curves and cell tropisms between rIHNV-N438A and rIHNV-N56A, rIHNV-N379A, rIHNV-N401A, rIHNV-N56A-N379A-N401A, rIHNV-N56A-N379A-N438A, so we inferred that mutation of the 438th amino acid in the G protein alone may lead to a change of the conformation of the G protein that differs from other forms of mutations, resulting in decreased viral pathogenicity of rIHNV-N438A. Moreover, the 438th amino acid is located in the neutralizing epitope area of the G protein, and its deglycosylation mutation would lead to exposure of the neutralization epitope, resulting in increased immunogenicity of rIHNV-N438A and early and high level production of IgM antibody with neutralizing activity. Thus, we could conclude that the decreased pathogenicity and increased immunogenicity of the rIHNV-N438A were related to high protection rate for fish against IHNV, highlighting a promising candidate for the development of anti-IHNV attenuated vaccine, but the specific mechanism needs further study.

In conclusion, we predicted four potential N-linked glycosylation sites at positions 56, 379, 401, and 438 of the IHNV G protein, and used this information to construct nine recombinant IHNVs with different levels of impaired glycosylation. Our results show that glycosylation impairment of the IHNV G protein affects viral pathogenicity and immunogenicity, provides a basis for the study of the mechanism of IHNV pathogenesis, and suggests a starting point for the development of a live-attenuated vaccine against IHNV.

Acknowledgements

This work was supported by the National Key R&D Program of China (2017YFD0501105).

Appendix A. Supplementary data

Supplementary data to this article can be found online at https://doi.org/10.1016/j.fsi.2019.04.038.

References

[1] P. Dixon, R. Paley, R. Alegria-Moran, B. Oidtmann, Epidemiological characteristics of infectious hematopoietic necrosis virus (IHNV): a review, Vet. Res. 47 (2016) 1–26.
[2] P.J. Enzmann, G. Kurath, D. Fichtner, S.M. Bergmann, Infectious hematopoietic necrosis virus: monophyletic origin of European isolates from North American genogroup M, Dis. Aquat. Org. 66 (2005) 187–195.
[3] S. Ahmadivand, M. Soltani, K. Mardani, S. Shokrpoor, R. Hassanzadeh, M. Ahmadpoor, H. Rahmati-Holasoo, S. Meshkini, Infectious hematopoietic necrosis virus (IHNV) outbreak in farmed rainbow trout in Iran: viral isolation, pathological findings, molecular confirmation, and genetic analysis, Virus Res. 229 (2017) 17–23.
[4] M. Alonso, J.A.C. Leong, Licensed DNA vaccines against infectious hematopoietic necrosis virus (IHNV), Recent Pat. DNA Gene Sequences 7 (2013) 62–65.
[5] A. Ammayappan, S.E. Lapatra, V.N. Vakharia, Molecular characterization of the virulent infectious hematopoietic necrosis virus (IHNV) strain 220-90, Virol. J. 7 (2010) 1–11.
[6] R. Assenberg, O. Delmas, B. Morin, S.C. Graham, X. De Lamballerie, C. Laubert, B. Coutard, J.M. Grimes, J. Neyts, R.J. Owens, B.W. Brandt, A. Gorbalenya, P. Tucker, D.I. Stuart, B. Canard, H. Bourhy, Genomics and structure function studies of *Rhabdoviridae* proteins involved in replication and transcription, Antivir. Res. 87 (2010) 149–161.
[7] C. Wang, L.L. Zhao, Y.J. Li, L.J. Tang, X.Y. Qiao, Y.P. Jiang, M. Liu, Analysis of the genome sequence of infectious hematopoietic necrosis virus HLJ-09 in China, Virus Gene. 52 (2016) 1–9.
[8] Y. Wu, M.T. Guo, X.J. Hua, K.X. Duan, G.H.34 Lian, L. Sun, L.J. Tang, Y.G. Xu, M. Liu, Y.J. Li, The role of infectious hematopoietic necrosis virus (IHNV) proteins in the modulation of NF-kappaB pathway during IHNV infection, Fish Shellfish Immunol. 63 (2017) 500–506.
[9] V. Noel, L.O. Ei, N. Tomonori, K. Hidehiro, H. Ikuo, A. Takashi, K. Hiroshi, Y. Yoshikazu, A soluble nonglycosylated recombinant infectious hematopoietic necrosis virus (IHNV) G-protein induces IFNs in rainbow trout (Oncorhynchus mykiss), Fish Shellfish Immunol. 25 (2008) 170–180.
[10] H.M. Engelking, J.C. Leong, The glycoprotein of infectious hematopoietic necrosis virus elicits neutralizing antibody and protective responses, Virus Res. 13 (1989) 213–230.
[11] P. Boudinot, M. Blanco, P. de Kinkelin, A. Benmansour, Combined DNA immunization with the glycoprotein gene of viral hemorrhagic septicemia virus and infectious hematopoietic necrosis virus induces double-specific protective immunity and non specific response in rainbow trout, Virology 249 (1998) 297–306.
[12] C.H. Kim, J.R. Winton, J.C. Leong, Neutralization-resistant variants of infectious hematopoietic necrosis virus have altered virulence and tissue tropism, J. Virol. 68 (1994) 8447–8453.
[13] C. Huang, M.S. Chien, M. Landolt, W. Batts, J. Winton, Mapping the neutralizing epitopes on the glycoprotein of infectious haematopoietic necrosis virus, a fish rhabdovirus, J. Gen. Virol. 77 (1996) 3033–3040.
[14] S.E. LaPatra, C. Evilia, V. Winston, Positively selected sites on the surface glycoprotein (G) of infectious hematopoietic necrosis virus, J. Gen. Virol. 89 (2008) 703–708.
[15] A.G. Pletnev, M. Bray, C.J. Lai, Chimeric tick-borne encephalitis and dengue type 4 viruses: effects of mutations on neurovirulence in mice, J. Virol. 67 (1993) 4956–4963.
[16] V. Vorndam, J.H. Mathews, A.D. Barrett, J.T. Roehrig, D.W. Trent, Molecular and biological characterization of a non-glycosylated isolate of St Louis encephalitis virus, J. Gen. Virol. 74 (1993) 2653–2660.
[17] G.R. Risatti, L.G. Holinka, I.F. Sainz, C. Carrillo, Z. Lu, M.V. Borca, N-linked glycosylation status of classical swine fever virus strain Brescia E2 glycoprotein influences virulence in swine, J. Virol. 81 (2007) 924–933.
[18] C. Soowannayan, N. Chanarpakorn, M. Phanthura, N. Deekhlai, C. Kunasol, S. Sriurairatana, N-Linked glycosylation is essential for the yellow head virus replication cycle, J. Gen. Virol. 94 (2013) 2458–2468.
[19] X. Shi, R.M. Elliott, Analysis of N-Linked glycosylation of hantaan virus glycoproteins and the role of oligosaccharide side chains in protein folding and intracellular trafficking, J. Virol. 78 (2004) 5414–5422.
[20] F. Zheng, L. Ma, L. Shao, G. Wang, F. Chen, Y. Zhang, S. Yang, Defining the N-linked glycosylation site of hantaan virus envelope glycoproteins essential for cell fusion, J. Microbiol. 46 (2008) 233.
[21] D. Zhao, L. Liang, S. Wang, T. Nakao, Y. Li, L. Liu, Y. Guan, S. Fukuyama, Z. Bu, Y. Kawaoka, H. Chen, Glycosylation of the hemagglutinin protein of H5N1 influenza virus increases its virulence in mice by exacerbating the host immune response, J. Virol. 91 (2017) e02215–e02216.
[22] J.N. Reitter, R.E. Means, R.C. Desrosiers, A role for carbohydrates in immune evasion in AIDS, Nat. Med. 4 (1998) 679–684.
[23] J. Lee, J.S. Park, J.Y. Moon, K.Y. Kim, H.M. Moon, The influence of glycosylation on secretion, stability, and immunogenicity of recombinant HBV pre-S antigen synthesized in *Saccharomyces cerevisiae*, Biochem. Biophys. Res. Commun. 303 (2003) 427–432.
[24] I.H. Ansari, B. Kwon, F.A. Osorio, A.K. Pattnaik, Influence of N-linked glycosylation

of porcine reproductive and respiratory syndrome virus GP5 on virus infectivity, antigenicity, and ability to induce neutralizing antibodies, J. Virol. 80 (2006) 3994–4004.
[25] C. Wang, G.H. Lian, L.L. Zhao, Y. Wu, Y.J. Li, L.J. Tang, X.Y. Qiao, Y.P. Jiang, M. Liu, Virulence and serological studies of recombinant infectious hematopoietic necrosis virus (IHNV) in rainbow trout, Virus Res. 220 (2016) 193–202.
[26] P. de Kinkelin, M. Bearzotti, J. Castric, P. Nougayrede, F. Lecocq-Xhonneux, M. Thiry, Eighteen years of vaccination against viral haemorrhagic septicaemia in France, Vet. Res. 26 (1995) 379–387.
[27] S.S. Ristow, S.E. LaPatra, R. Dixon, C.R. Pedrow, W.D. Shewmaker, J.W. Park, G.H. Thorgaard, Responses of cloned rainbow trout *Oncorhynchus mykiss* to an attenuated strain of infectious hematopoietic necrosis virus, Dis. Aquat. Org. 42 (2000) 163–172.
[28] M. Fernandez-Alonso, A. Rocha, J.M. Coll, DNA vaccination by immersion and ultrasound to trout viral haemorrhagic septicaemia virus, Vaccine 19 (2001) 3067–3075.
[29] N.A. Ballesteros, M. Alonso, S.R. Saint-Jean, S.I. Perez-Prieto, An oral DNA vaccine against infectious haematopoietic necrosis virus (IHNV) encapsulated in alginate microspheres induces dose-dependent immune responses and significant protection in rainbow trout (Oncorrhynchus mykiss), Fish, Shellfish Immunol 45 (2015) 877–888.
[30] S. Biacchesi, M.I. Thoulouze, M. Bearzotti, Y.X. Yu, M. Bremont, Recovery of NV knockout infectious hematopoietic necrosis virus expressing foreign genes, J. Virol. 74 (2000) 11247–11253.
[31] S. Biacchesi, M. Bearzotti, E. Bouguyon, M. Bremont, Heterologous exchanges of the glycoprotein and the matrix protein in a Novirhabdovirus, J. Virol. 76 (2002) 2881–2889.
[32] A. Ammayappan, S.E. LaPatra, V.N. Vakharia, A vaccinia-virus-free reverse genetics system for infectious hematopoietic necrosis virus, J. Virol Methods 167 (2010) 132–139.
[33] E.J. Emmenegger, S. Biacchesi, E. Merour, J.A. Glenn, A.D. Palmer, M. Bremont, G. Kurath, Virulence of a chimeric recombinant infectious haematopoietic necrosis virus expressing the spring viraemia of carp virus glycoprotein in salmonid and cyprinid fish, J. Fish Dis. 41 (2018) 67–78.
[34] I.C. Lorenz, J. Kartenbeck, A. Mezzacasa, S.L. Allison, F.X. Heinz, A. Helenius, Intracellular assembly and secretion of recombinant subviral particles from tick-borne encephalitis virus, J. Virol. 77 (2003) 4370–4382.